Impact of the Spring Distraction System on scoliotic spine morphology: an MRI- and CT-based analysis

Nick de Block
N.deblock@umcutrecht.nl

UMC Utrecht, The Netherlands
Student ID: 5854423
Supervisors: Casper S. Tabeling &
Prof. Dr. M.C. Kruijt
Orthopedics department

May 22, 2023
-
August 26, 2023

Study Design
Prospective cohort study

Summary of Background Information
Early Onset Scoliosis (EOS) is a three-dimensional (3D) deformation of the spine and trunk below the age of 10, which can lead to pulmonary insufficiency and even death. At UMC Utrecht, the Spring Distraction System (SDS) was developed to provide dynamic and continuous reduction of the scoliotic spine while allowing for near-physiological spinal growth. This study investigated morphometric differences in the intervertebral discs (IVDs) and vertebral bodies (VBs) before and at an average of 1.5 years after SDS implantation surgery in a prospective study cohort. For this analysis, MRI imaging and CT-based imaging was used to assess the 3D shape of individual IVDs and VBs, as well as of the relative position of the nucleus pulposus (NP) in the annulus fibrosus.

Methods
3D morphology of peri-apical levels of ten EOS patients were compared before surgery and at least 1-year after surgery using MRI- and CT-based imaging. Peri-apical VBs and IVDs were semi-automatically segmented to determine the lengths of the anterior, posterior, convex and concave aspects of these structures, as well as their rotation, while taking their 3D-orientation into account. Additionally, NP morphology was analyzed using MRI-based IVD reconstructions.

Results
Primary thoracic curves showed a height increase in every segment, except for the IVD convexity, with a mean gain of 7.6 ± 3.1 mm. This increase was mainly seen in the VB (7.0 ± 5.2 mm), compared to the IVD (0.6 ± 3.1 mm) Relative changes were most prevalent along both the VB and IVD concavity showing 17% and 13% height increase respectively, compared to 11% and -6% in the convexity.
Reduction of the deformity was mainly seen in the IVD where concave/convex length ratios normalized from 0.65 to 0.80, translating to 5.9 mm of coronal wedging reduction. Anterior/posterior ratios normalized from 1.25 to 1.21, indicating less lordosis. The VB also showed wedging reduction, but to a much lesser extent. Here, concave/convex ratios normalized from 0.85 to 0.89, indicating a 1.8 mm coronal correction, however anterior/posterior ratios increased from 0.97 to 1.00.

Both VB and IVD rotation appeared stable pre- versus post-surgery showing a positive correlation between rotational severity and (peri-)apical level.

The NP center of volume showed a pre-surgery mean distance to the IVD center of volume of 4.4 ± 1.1 mm. This distance decreased to 2.6 ± 1.0 mm post-surgery.

Conclusion
The reduction of scoliotic spines in EOS patients using the SDS results in a transition towards a more physiological shape, affecting both IVD and VB morphology. Most correction of the deformity takes place in the IVD while the spine continues to grow in the VBs. A trend is shown where this bony growth is modulated, resulting in decreased coronal wedging. Additionally, a trend is observed where the NP takes on a more centralized position in the IVD.

List of abbreviations

EOS	Early Onset Scoliosis	VB	Vertebral body
SDS	Spring Distraction System	IVD	Intervertebral disc
3D	Three-dimensional	NP	Nucleus Pulposus

1. Introduction

Early onset scoliosis (EOS) is a rare condition resulting in a three-dimensional (3D) deformation of the spine and trunk. EOS can result in thoracic insufficiency, respiratory failure and possibly even death if left untreated.[1,2] Its etiology is varied as there are several groups of diseases that can cause this condition. Due to EOS specifically affecting young children, it is always progressive in nature and timely intervention is therefore essential.[3] Key treatment goals are to reduce the spine to its original anatomical shape, to allow proper thoracic and pulmonary development, while minimizing the need for hospitalization and the risk of complications.[4,5]

Serial (Mehta) casting can cure EOS completely, however, only in the very young.[6] Bracing in older children is often unable to halt progression and surgery is then required to allow for adequate thoracic growth. Through the years, growth-friendly treatment options, such as traditional growing rods and vertical expendable prosthetic titanium ribs have been developed that attempt to reduce the spine to its original anatomical shape while allowing for unhindered growth.[7,8] A major downside to many of these interventions is the need for frequent re-operations to maintain adequate distraction force.[6] Although these are relatively minor surgeries, they can have a significant impact on both the patient, family and healthcare system.[9] Magnetically controlled growing rods were then introduced to allow for external distraction using magnets to bypass the need for invasive surgery. These implants are, however, accompanied by a high implant-related complication rate, frequent outpatient clinic visitations for further distraction and high risk for revision surgery.[1,9-14]

To address these issues, the spring distraction system (SDS) was developed [Figure 1], which uses compressed coil springs to apply continuous distraction forces on the spine. These springs are implanted around sliding rods that can move freely within a stacked connector frame that connects to a rigid rod providing stability to the implant.[14] As the spring applies continuous force on the spine there is no need for repeated lengthening procedures and the customizable nature of the implant allows for more personalized configurations to be created in order to more appropriately treat the scoliotic spine.[4,5,10-12]

Previous publications support the feasibility of this system as an alternative to other growing spine solutions as both curve growth and correction remained acceptable without the need for repetitive lengthening procedures.[5,10-12,16,17]

Actual effects of SDS on spine morphology remain unclear however. Hence, the aim of this study is to assess morphometric changes of both the vertebral bodies (VBs) and intervertebral discs (IVDs) pre- vs one-year post-surgery using MRI- and CT-based imaging.

2. Materials & methods

Study population

CT- and MRI-scans were selected from a prospective cohort in which the SDS is implanted in EOS patients. Inclusion criteria were having both pre- and at least one year post-operative MRI- or CT-based imaging. Exclusion criteria were re-operation with an implant configuration alteration that has taken place before the post-operative scan, incomplete scans where not all apical levels were visible and no primary thoracic curve.

Vertebral body and discus height measurements

For each patient, the apex of the scoliotic curve was identified and peri-apical levels were analyzed. This segment consists of two VBs above and below the curve apex, as well as adjacent IVDs. Dependent on whether the apex consists of a VB or IVD the length of the segment varies between five VBs and six IVDs or four VBs and five IVDs. This was done for both pre- and post-operative scans to assess the effects of the SDS. Previously validated software and semi-automatic image processing techniques for CT-scans of the scoliotic spine (ScoliosisAnalysis 7.2, Image Sciences Institute, Utrecht, the Netherlands) based on MeVisLab (MeVis Medical Solutions AG, Bremen, Germany), were used by one observer to provide complete 3D coordinate systems of the individual structures of all spines. This is done by segmenting all the upper and lower vertebral body endplates and the spinal canal in the 'true' transverse plane by correcting for the coronal and sagittal angulation of each endplate. [Figure 2]

A line corresponding with the true anterior-posterior axis (based on the centroids of the endplate and spinal canal) at the center of the endplate was used to localize the lateral and anterior-posterior borders of each endplate. The distances between the 3D coordinates of these points were automatically calculated, to get the total concave, convex, anterior and posterior lengths of included vertebral bodies and IVDs.[18] These aforementioned coordinates were then also used to calculate VB and IVD rotation per level. [*Mean(Arctan(Xdiff/Zdiff upper endplate)*(180/π));(arctan(Xdiff/Zdiff lower endplate)*(180/π))*] Length ratios were calculated as [*(mean anterior length)/(mean posterior length)]* and *[(mean concave length)/(mean convex length)*] for VB and IVD total segment lengths respectively.

Nucleus pulposus analysis

T2-weighted Sagittal MRI-scans with a general slice thickness of 3-4 mm were segmented using Mimics Innovation Suite 23.0 (Materialise, Leuven, Belgium) to make 3D-models of the IVDs. For each scan, all IVDs incorporated in the included segments were analyzed by one observer.

First, a mask corresponding with the nucleus pulposus (NP) was manually created. By fusing the masks that are made for each scan slice that incorporate the NP together, a reconstruction was created in 3D-space.

Second, the entire IVD was segmented manually by providing a secondary mask that covers this structure. These masks were then also fused and transformed into 3D-models and combined with the NP models to create a complete reconstruction of the included segment IVDs.

Third, the 3D IVD-models were exported to 3-Matic (v17.0, Materialise, Leuven, Belgium) software to perform a separate NP analysis to assess a possible shift of this structure within the IVD post-surgery. This was done by comparing the pre- and post-operative distances between the NP centers of volume, relative to the IVD centers of volume. [Figure 3]

Statistical analysis

The statistical analyses in this study were done in SPSS 27.0 for Windows (SPSS Inc., Chicago, IL). Descriptive statistics were computed providing means, ranges and standard deviations. Anterior-posterior and convex-concave length discrepancies, rotation, as well as nucleus position, pre- versus post-surgery were analyzed using paired sample t-tests. For the correlation between vertebral or disc rotation and peri-apical level a non-parametric Spearman's rho test was performed. Statistical significance level was set at 0.05. Potential outliers were identified and subset analyses were conducted to obtain more cohesive data.

3. Results

Study population

Ten out of 103 EOS patients aging from 4 to 15 were included. 93 patients were excluded: 9 due to poor image quality, 1 to short-follow up scan interval, 2 to re-operation, 4 to lumbar curves and 77 to a lack of imaging material. Patient and curve characteristics can be found in [Table 1].

Segmental lengths

Primary thoracic curves showed a length increase in every segment, except for the IVD convexity, with a mean increase of 7.6 ± 3.1 mm ($p < 0.000$). This increase was mainly seen in the VB (7.0 ± 5.2 mm; $p < 0.002$), compared to the IVD (0.6 ± 3.1 mm; $p < 0.559$). [Figure 4] Relative changes were most prevalent in both the VB and IVD concavity showing a 17% and 13% height increase respectively, compared to 11% and -6% in the convexity. This translated to a mean Cobb angle correction of 31° ± 13.1° ($p < 0.00$).

Length ratio alterations

Reduction of the deformity was mainly seen in the IVD [Figure 5] where concave/convex length ratios normalized from 0.65 to 0.80 ($p = 0.011$), which translates to an absolute wedging reduction in the coronal plane of 5.9 mm. Anterior/posterior ratios normalized from 1.25 to 1.21 ($p = 0.489$). The VB contributed to the reduction of the overall wedging, but to a much lesser extent. Here, concave/convex ratios normalized from 0.85 to 0.89 ($p = 0.112$), indicating a mean 1.8 mm correction, however anterior/posterior ratios increased from 0.97 to 1.00 ($p = 0.378$).

Subset analysis – Segmental lengths

A subset analysis was performed excluding patient SP69, which appeared to be an outlier based on general reversed findings shown in red in [Figure 6]. There was a mean length increase of 8.0 ± 3.0 mm ($p < 0.000$). This increase was mainly seen in the VB (7.5 ± 5.3 mm; $p = 0.003$), compared to the IVD (0.5 ± 3.3 mm; $p = 0.655$). [Figure 7] Relative changes were most prevalent in both the VB and IVD

concavity showing a 18% and 16% height increase respectively, compared to 11% and -8% in the convexity. This translated to a mean Cobb angle correction of 34° ± 8.7° ($p < 0.000$).

Subset analysis – Length ratio alterations

IVD concave/convex length ratios normalized from 0.64 to 0.82 ($p < 0.000$), showing a mean wedging reduction in the coronal plane of 7.6 mm. Anterior/posterior ratios remained unchanged. The VB showed concave/convex ratio decrease from 0.87 to 0.92 ($p = 0.007$), indicating a mean 2.6 mm correction. Anterior/posterior ratios remained stable at 0.97 ($p = 0.974$). [Figure 8]

Nucleus pulposus shift

The NP center of mass showed a pre-operative mean distance to the IVD center of mass of 4.3 ± 1.4 mm. This distance decreased to 2.6 ± 1.5 mm post-operatively [Figure 9] which translates to a 1.7 ± 1.1 mm ($p = 0.008$) As SP13, SP26 and SP69 had CT-based imaging, these patients were not included in this analysis.

Spinal rotation

Rotational shifts of both VBs and IVDs are displayed in [Figure 10]. Overall, VB rotation increased from 22.1° ± 8.8° to 23.1° ± 9.9° ($p = 0.442$). IVD rotation decreased from 22.2° ± 9.0° to 20.4° ± 8.1° ($p = 0.442$). After stratifying for (peri-) apical level into three groups [Figure 11]: apical, apex +1 and apex +2 the rotational differences per group were compared. Both pre-surgery VB rotation ($p = 0.04$) and post-surgery IVD rotation ($p = 0.009$) correlated significantly with their level relative to the curve apex.

Subset analysis – spinal rotation

Rotational shift subset analysis excluding patient SP26 is shown in [Figure 12]. Both VB (22.3° ± 9.3°-> 22.3° ± 9.5°; $p = 0.983$) and IVD (21.1° ± 8.8°-> 20.7° ± 8.5°; $p = 0.798$) rotation remained stable when comparing pre- versus post-surgery measurements. A significant correlation between VB and IVD rotation and level relative to the curve apex persisted ($p < 0.05$).

4. Discussion

The objective of this study was to assess the effect that SDS has on IVD and VB morphology by comparing the contributions of these structures to overall spine length. To the best of our knowledge, this is the first study to analyze the morphological changes in spines that have undergone growth-friendly implant surgery.

Length discrepancies in scoliotic spines compared to controls have been observed in several recent studies.[18,19] Generally, these discrepancies are present as a relative anterior lengthening, which is mostly prevalent in the IVDs and wedging of both the IVDs and VBs.[19-21] It has been described in several studies that VB wedging is either the result of asymmetrical growth or bone remodeling, dependent on the age of the subject.[22,23] As EOS patients are by definition young, this asymmetrical growth is a possible therapy target. Procedures such as tethering for example demonstrate growth modulation, where growth along the convexity is limited while concave growth continues. This results in a general curve correction

due to differential VB growth.[24,25] While there are several studies that analyze this phenomenon in tethering patients, there is a clear lack of such research on growth-friendly implants, such as the SDS. While volumetric studies have been done analyzing VB volume and overall height and depth after magnetically controlled growing rods implantation, a more detailed morphometric analysis remains absent.[26] This study suggests that possibly as a result of the continuous distraction forces, bony growth appears to be modulated. This results in decreased coronal vertebral wedging, as well as reduced lordosis, while allowing for near-normal spinal growth.

There are several points of interest to take away from the present data. As seen in [figure 6] patient SP69 shows vastly different length ratios compared to the overall study population. This observation could be related to unresolved implant failure that was observed four months prior to the CT-scan taken 1.8 years post-surgery. Due to this failure, the mobile rod was freed from its cranial cages, effectively nullifying the distraction forces on the concave spinal segment. Whilst the Cobb angle appeared stable at 55°, the negative sagittal balance had increased, potentially affecting overall findings. This is reflected in the additional subset analysis where this patient was excluded. In this analysis there is a larger reduction of coronal wedging and greater statistical significance for nearly all morphological changes.

Interestingly, a mean increase in disc height is observed and, albeit a minor one, this finding contradicts earlier studies that state that craniocaudal thoracic disc growth halts after the age of four in a healthy population.[27,28] Therefore, it can be assumed that this alteration to the disc shape is most likely a result of the continuous distraction forces that the SDS induces on the spine. It remains unclear whether these morphological changes are elastic or plastic in nature. Further research will have to be done to clarify the nature of these changes and their potential role in restoring spinal harmony.

Another interesting finding is seen in the rotational analysis of patient SP26. This patient showed a prevalent inverse linear correlation between the rotation of the VBs and the IVDs. It remains unclear what caused this singular finding that is not reflected in the rest of the study population. Additionally, compared to the other analyses, the rotational analysis showed clear inverse differences between several patient groups without a clear explanation. Overall, there does appear to be a correlation between the rotation and the (peri-)apical level, which has been described in previous studies.[29]

There are several limitations to this study. Firstly, as there is a very limited number of patients eligible for inclusion, the statistical power of this study is relatively poor. Furthermore, the study population itself is quite heterogenous due to varying causes of EOS and a great variation in age, possibly affecting study results. Moreover, as both MRI- and CT-based imaging were used to acquire data, analysis findings potentially differ between inclusions as the segmentation software is originally created and validated for CT-based imaging. This is reflected in the apparent outliers that were observed in several different analyses. Excluding these outliers for several subset analyses provides data which quite frequently shows statistical significance. However, as stated earlier, the overall statistical power of this study is quite poor and as a result, these findings should only be interpreted as general trends that could be used as starting hypotheses for future studies.

Secondly, while the IVD and NP analysis shows a trend where the NP centralizes in the disc, this finding was based on suboptimal measurement methods. T2-weighted sagittal MRI imaging were used to analyze the IVDs. However, as these scans have a general slice thickness of 3-4 mm, a large portion of especially the NP volume is potentially lost due to unfavorable slice positioning. This issue could be mitigated by making use of lower slice thickness MRI-scans, however this proves difficult as this pediatric patient population is prone to inducing movement artefacts during scan acquisition. As such, scan acquisition time is generally minimized to counter this issue resulting in suboptimal imaging to analyze. In addition to this, the software used proves to be suboptimal for scoliotic spine analysis. Normally this process could be executed in a semi-automatic manner by providing mask gray value upper and lower thresholds to specifically target the NP. This was however not possible in the scoliotic spine. As there is great overlap between the gray values of several spinal structures, adjustments have to be made to specifically identify the NP in the annulus fibrosus. This is especially prevalent in the scoliotic spine, where overall IVD and NP morphology are majorly affected.[30] Hence, a completely manual approach proved to be a superior analysis method, which could have induced greater inter-observer variability.

Thirdly, as MRI-based imaging is prone to be affected by metal implants the actual quality of these scans is subject for discussion. Whilst at first glance these scans appeared usable for analysis [Figure 13], the actual effects of implant artefacts on overall image quality and thereby observer interpretability was not accounted for by repeating the segmentation process or having a second blinded observer do the same analyses. Originally, the goal of this study was to make use of bone-MRI-based synthetic CT-scans to provide more adequate segmentation of the VBs, possibly allowing for more accurate data to be acquired, however these images are not available for analysis yet.

5. Conclusion

The SDS appears to reduce the scoliotic spine in EOS patients to a more physiological shape, affecting both IVD and VB morphology. Most correction of the deformity was seen in the IVD, where coronal wedging was greatly reduced. This decreased wedging was however, also observed in the VBs where bony growth appears to be modulated by the altered forces on the spine. Both VB and IVD rotation appeared stable pre- versus post-surgery showing a positive correlation between rotational severity and (peri-)apical level. Additionally, a trend was observed where the NP shifts to a more centralized position in the IVD, possibly playing a role in restoring spinal harmony.

Figures and tables

Figure 1. The Spring Distraction System. Current SDS configuration with three components added to 5.5mm Cobalt-Chromium (CoCr) rods: two parallel side-to-side connectors (green) with one oversized hole that was kept unlocked, a compressed titanium (Ti6Al4V) spring (gold) that provides either 50, 75 or 100 N of distraction force and a locking buttress (blue)

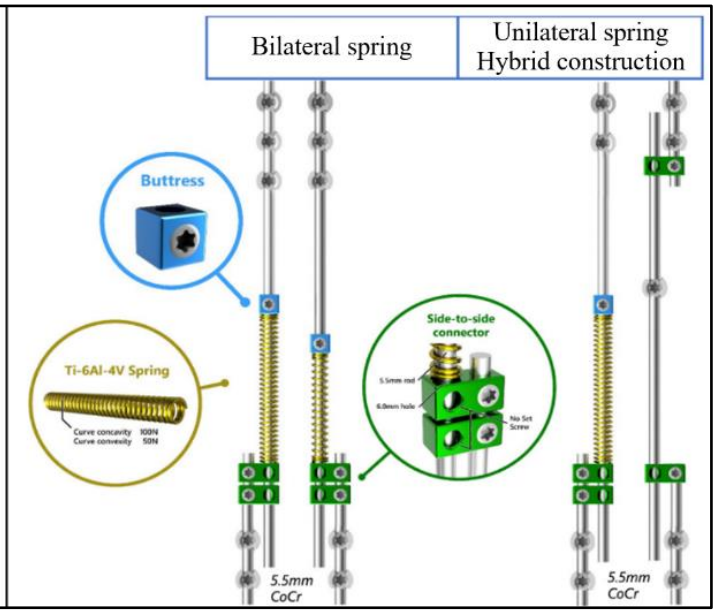

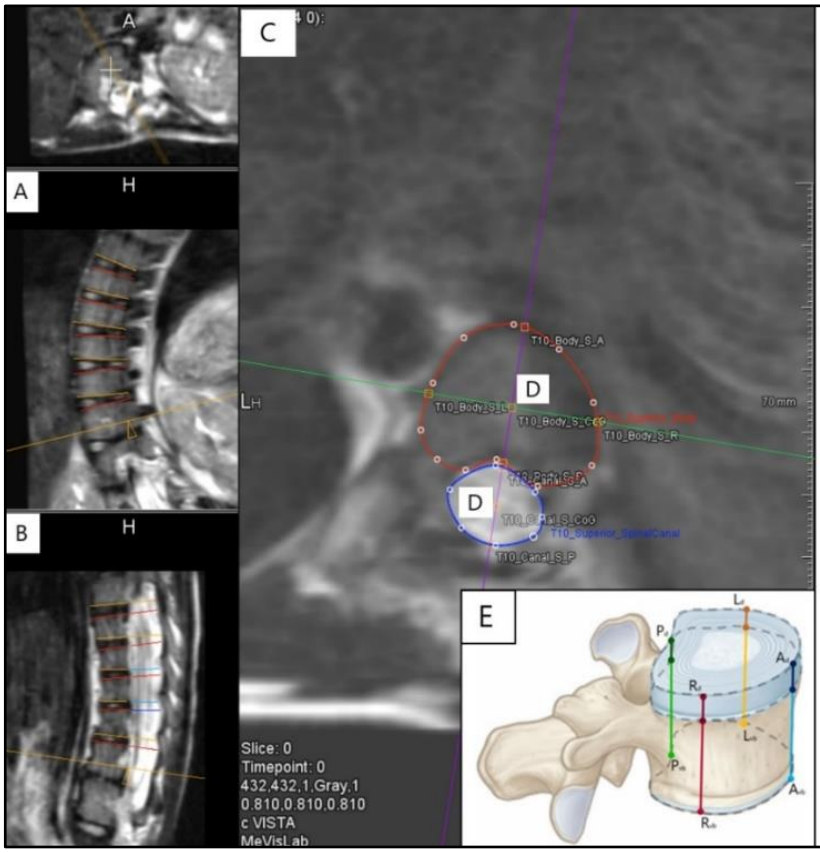

Fig. 2. Segmentation process of a T10 superior endplate using ScoliosisAnalysis software.
By drawing lines that correct for coronal (A) and sagittal (B) tilt of each endplate, a true axial view (C) is acquired.
In this plane, the endplate (red) and spinal canal (blue) were manually segmented and the centroids (D) of these structures were automatically calculated.
Using these centroids, a true midsagittal plane (purple line) and perpendicular to this axis at the VB centroid a true coronal plane (green line) are computed.
Where these axis meet the segmentation of the VB, anterior, posterior, left and right points are drawn. Distances between the 3D coordinates of these points are automatically calculated (E – schematic representation), to get the total concave, convex, anterior and posterior lengths of included segments.

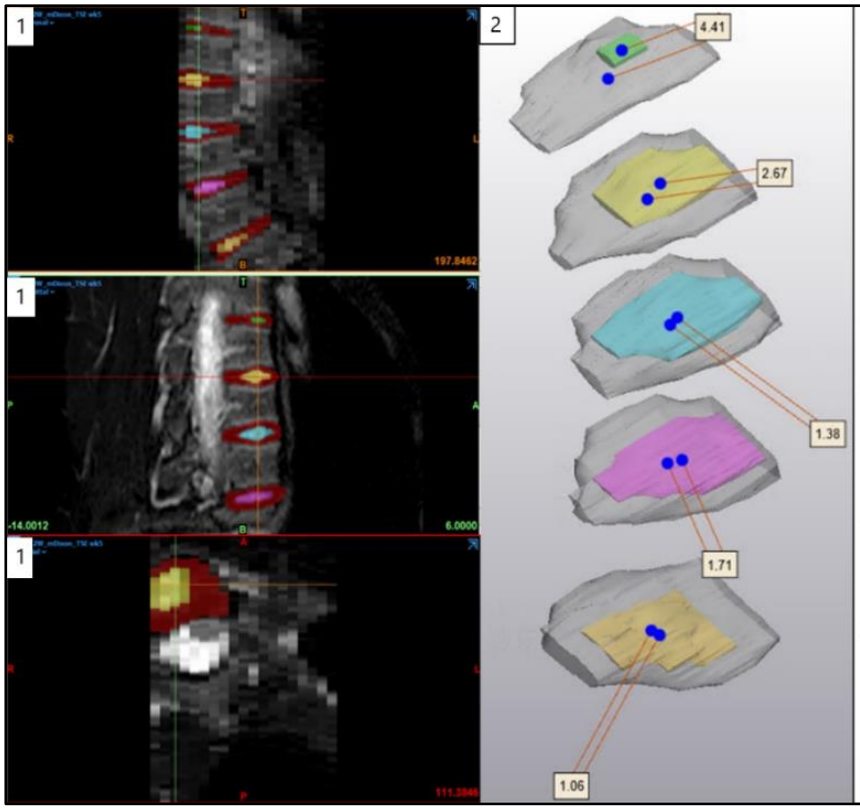

Figure 3. IVD nucleus analysis using MIMICS (left) and 3-Matic software (right).
(1) By manually creating masks per scan slice that cover either a NP (pink for example) or the whole IVD (red) specifically, a 3D-model is reconstructed by fusing these slice masks together.
(2) This 3D-model is exported to 3-Matic where IVD and NP centers of volume are semi-automatically calculated. The distances between these points are then semi-automatically measured.

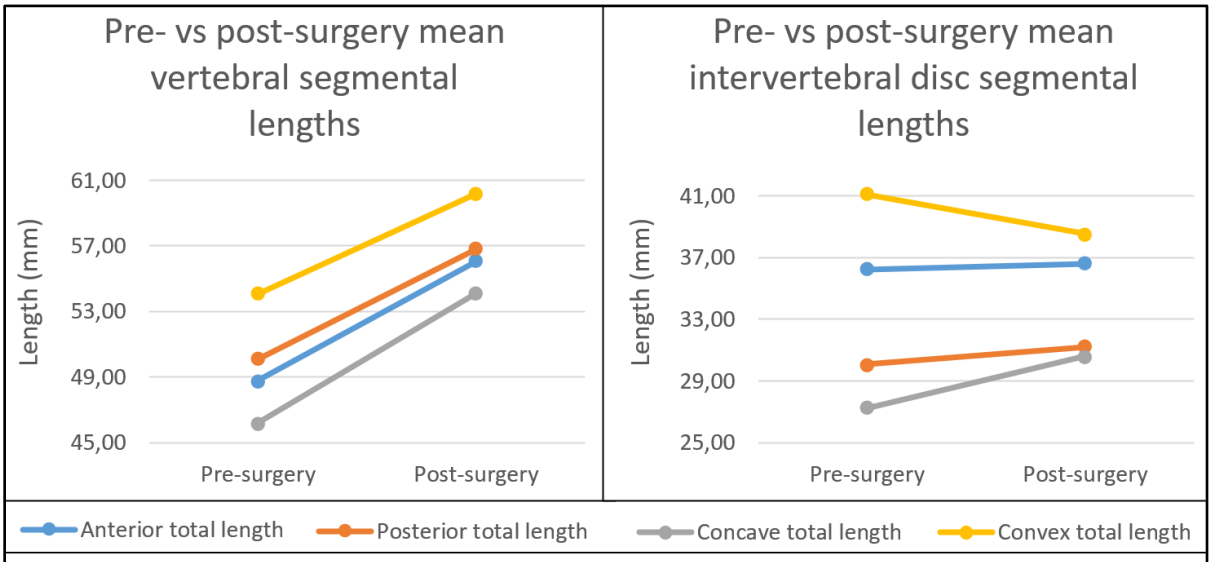

Figure 4. Mean pre- versus post-surgery vertebral body and intervertebral disc segmental lengths

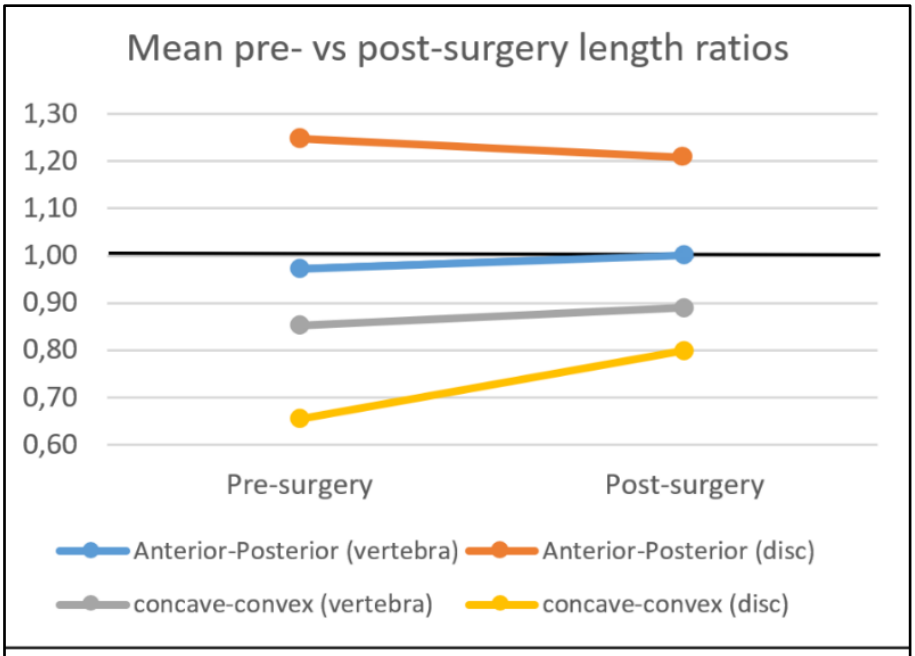

Figure 5. Mean pre- versus post-surgery anterior-posterior and concave-convex vertebral body and intervertebral disc length ratios

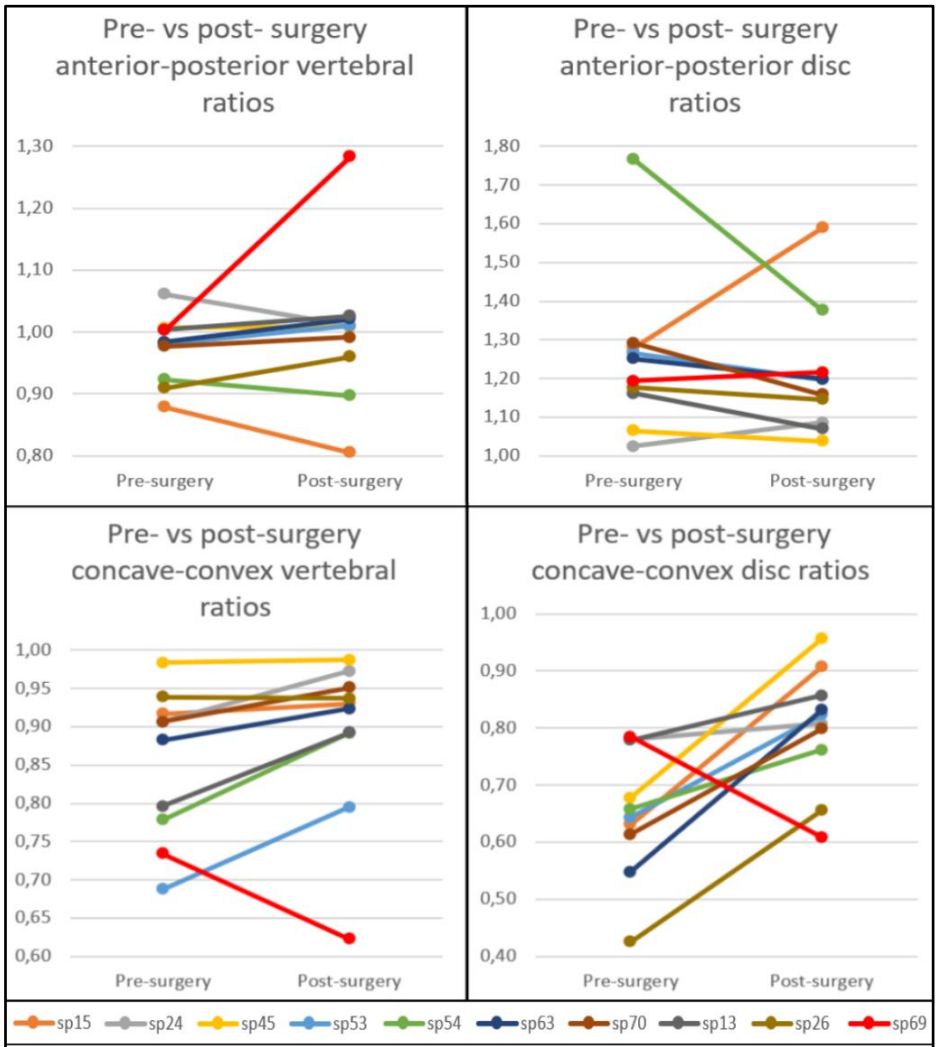

Figure 6. Overview of pre- versus post-surgery anterior-posterior and concave-convex segmental length ratios for vertebral bodies and intervertebral discs respectively

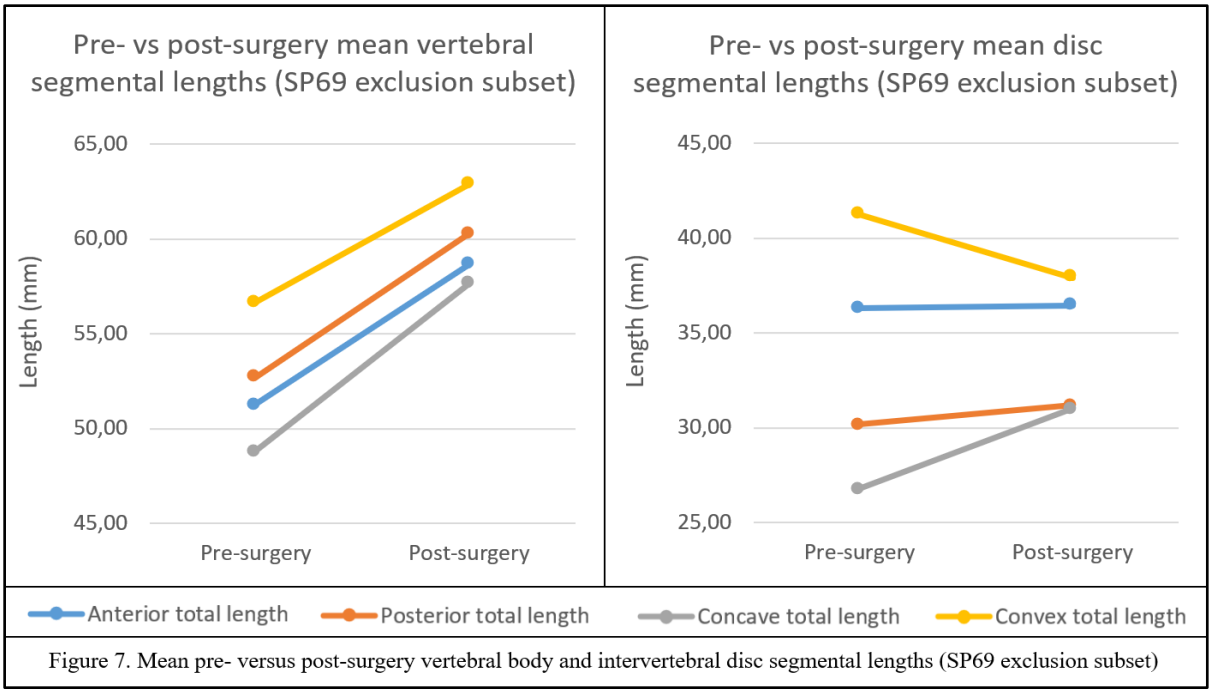

Figure 7. Mean pre- versus post-surgery vertebral body and intervertebral disc segmental lengths (SP69 exclusion subset)

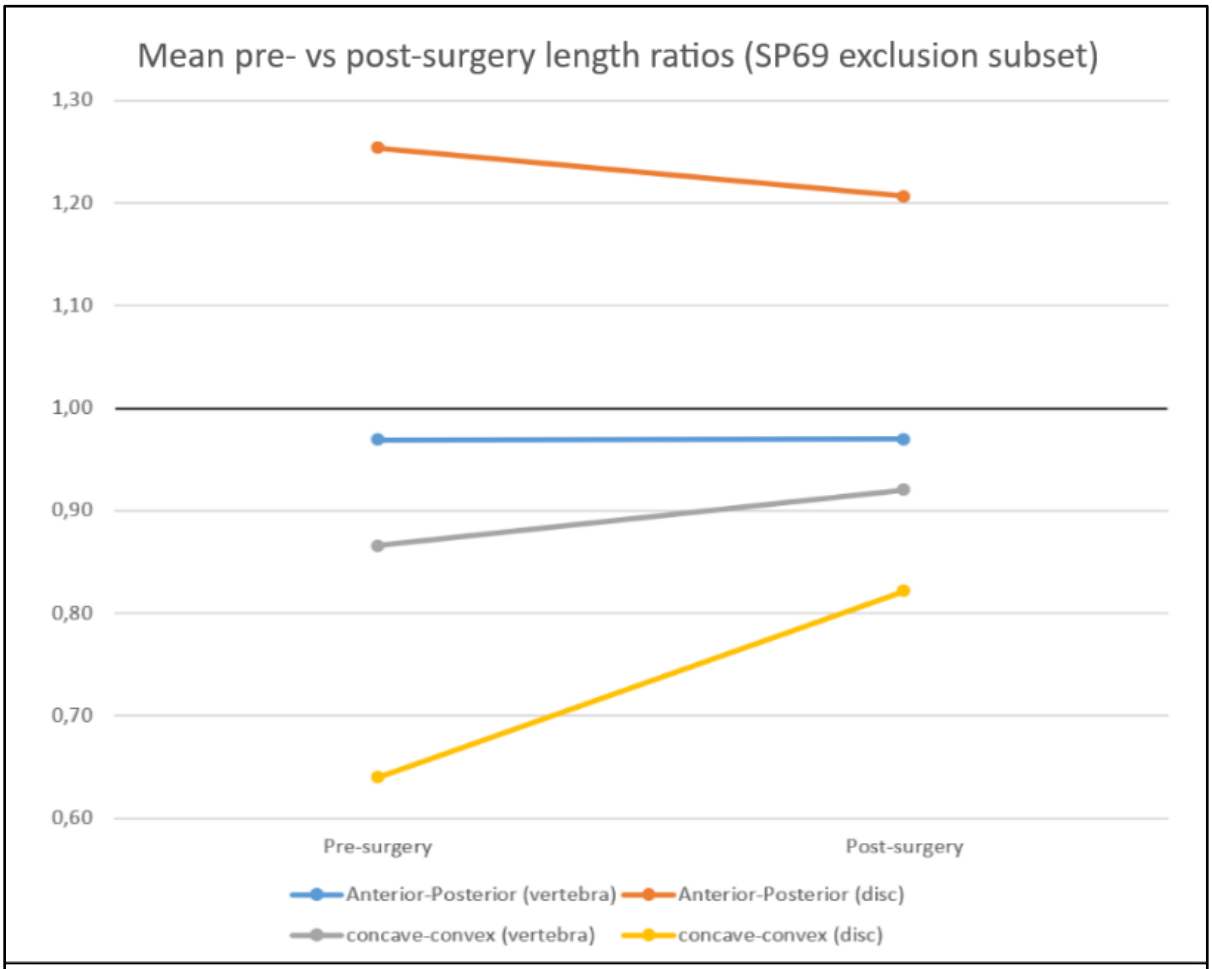

Figure 8. Mean pre- versus post-surgery anterio-posterior and concave-convex vertebral body and intervertebral disc length ratios (SP69 exclusion subset)

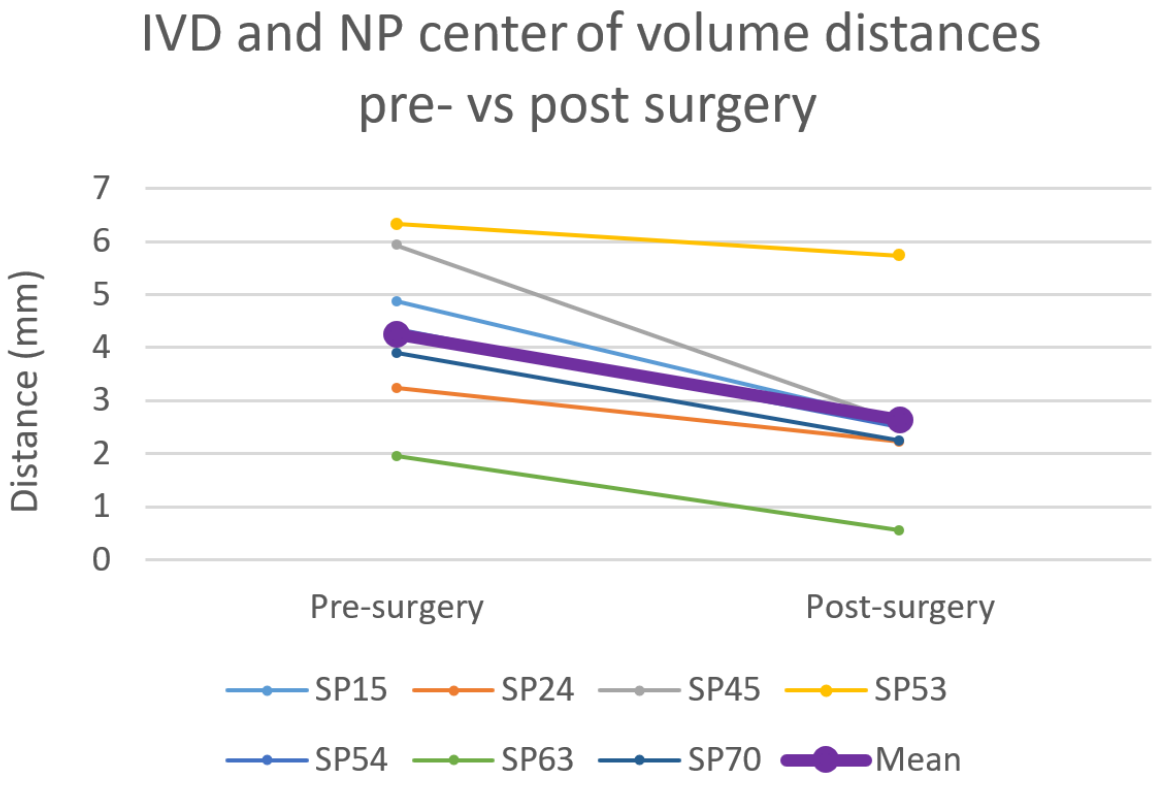

Figure 9. Overview of pre- versus post-surgery intervertebral disc and nucleus pulposus center of volume distances

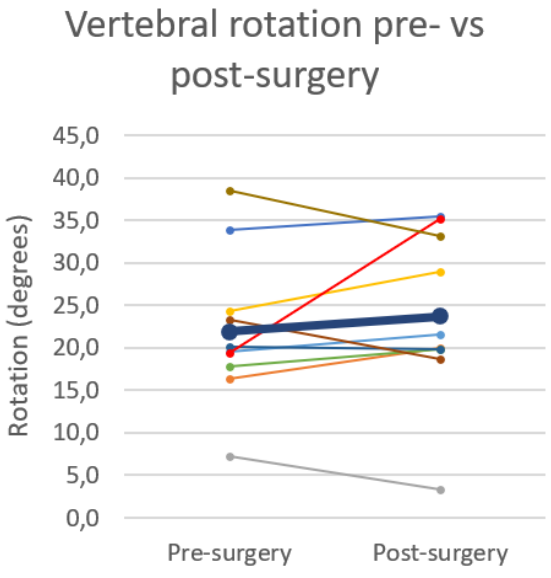

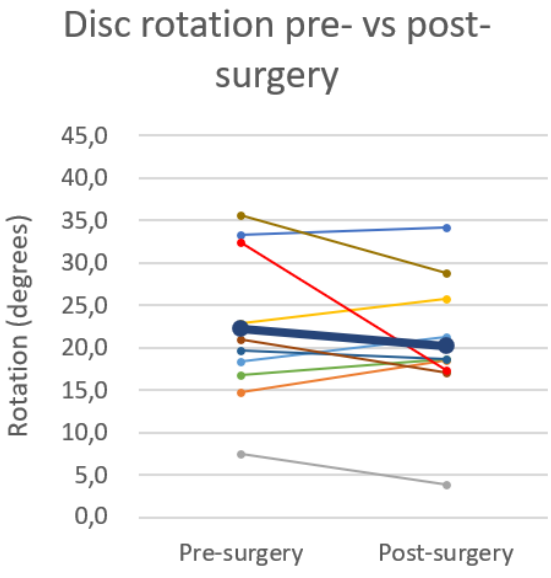

Figure 10. Pre- versus post-surgery vertebral body and intervertebral disc rotation

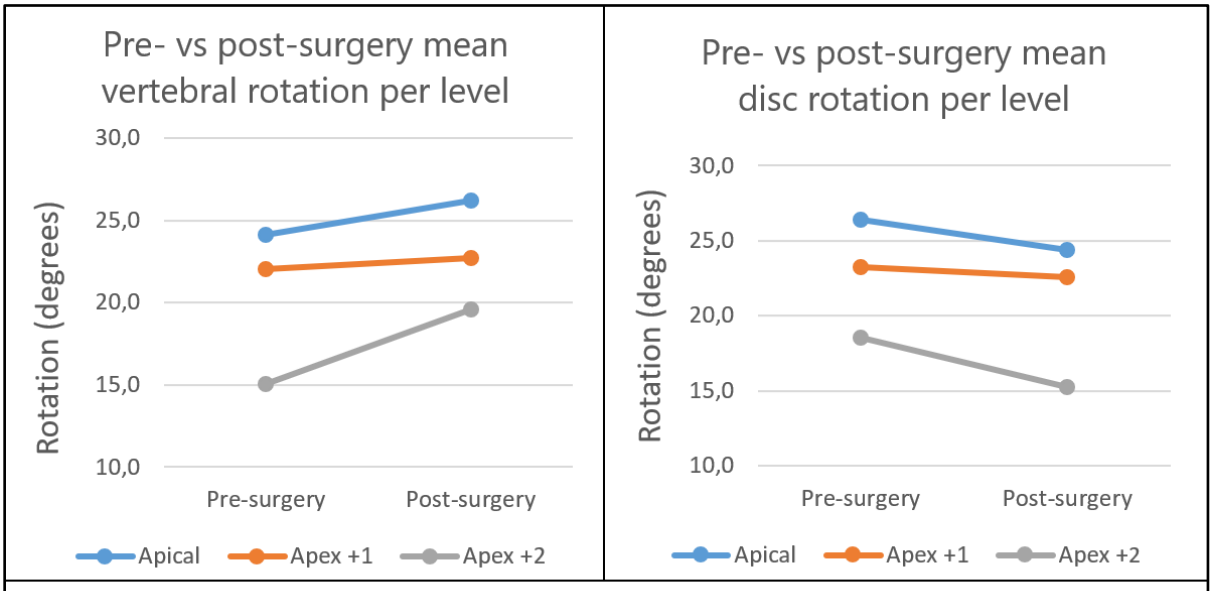

Figure 11. Mean pre- versus post-surgery vertebral body and intervertebral disc rotation per peri-apical level

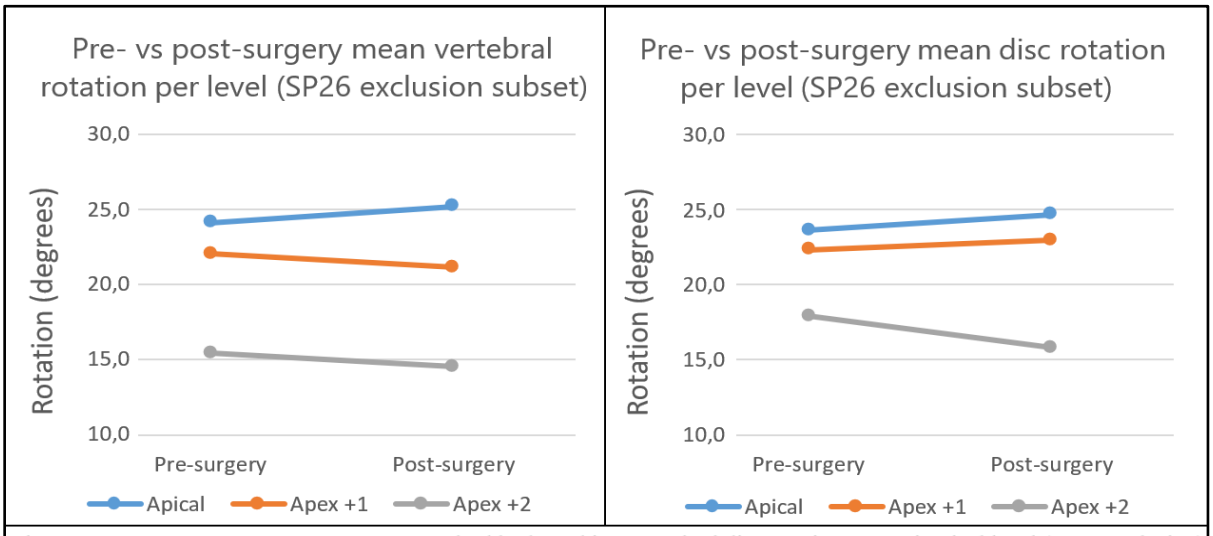

Figure 12. Mean pre- versus post-surgery vertebral body and intervertebral disc rotation per peri-apical level (SP26 exclusion)

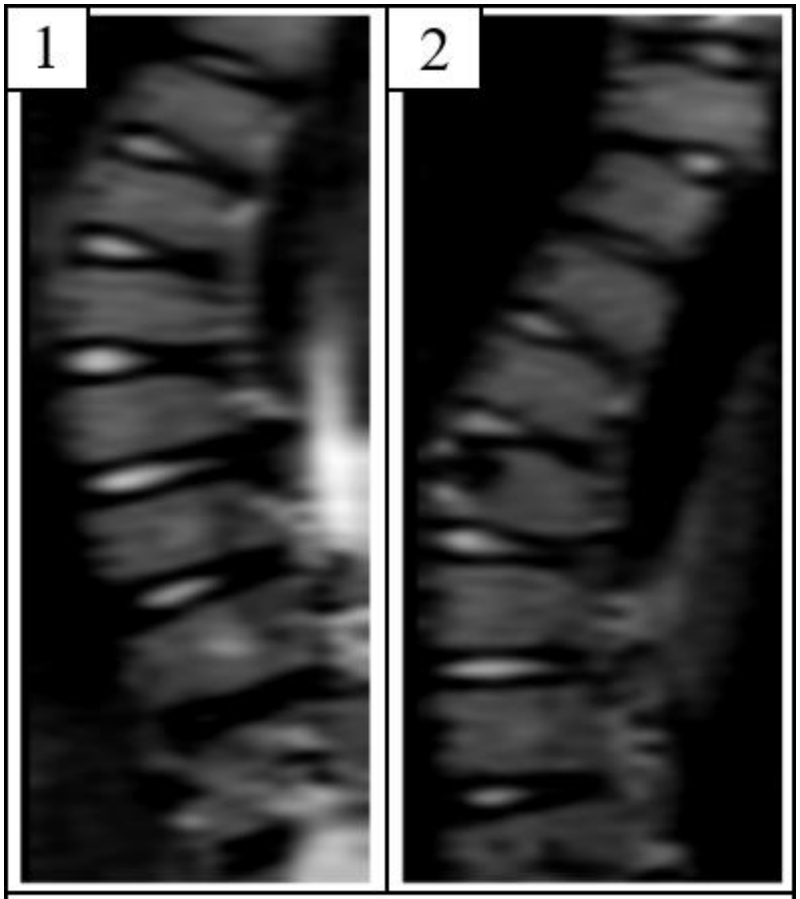

Figure 13. Comparison of pre-surgery (1) versus post-surgery (2) MRI-image quality

Table 1. Study population characteristics	
	SDS patients (*n = 10*)
MRI	7 (70%)
CT	3 (30%)
Age (Mean)± SD	9.1 (± 3.6)
Girls	3 (30%)
Rightsided curve convexity	9 (90%)
Mean Cobb angle ± SD	69.2° (± 12.1)
Apex level	
T4-T5	1 (10%)
T6-T7	1 (10%)
T7-T8	3 (30%)
T8-T9	3 (30%)
T9-T10	2 (20%)
Disc as apex	7 (70%)

Literature

1. Campbell RM Jr, Smith MD, Mayes TC, Mangos JA, Willey-Courand DB et al. The characteristics of thoracic insufficiency syndrome associated with fused ribs and congenital scoliosis. J Bone Joint Surg Am. 2003 Mar;85(3):399-408.

2. Wang, Y., Wang, D., Zhang, G. *et al.* Effects of spinal deformities on lung development in children: a review. *J Orthop Surg Res* 18, 246 (2023).

3. Ruiz G, Torres-Lugo NJ, Marrero-Ortiz P, Guzmán H, Olivella G, Ramírez N. Early-onset scoliosis: a narrative review. EFORT Open Rev. 2022 Aug 4;7(8):599-610.

4. Tabeling CS, Lemans JVC, Top A, Scholten EP, Stempels HW, et al. The Spring Distraction System for Growth-Friendly Surgical Treatment of Early Onset Scoliosis: A Preliminary Report on Clinical Results and Safety after Design Iterations in a Prospective Clinical Trial. J Clin Med. 2022 Jun 28;11(13):3747.

5. Lemans JVC, Wijdicks SPJ, Castelein RM, Kruyt MC. Spring distraction system for dynamic growth guidance of early onset scoliosis: two-year prospective follow-up of 24 patients. Spine J. 2021 Apr;21(4):671-681.

6. Montgomery BK, Tileston K, Kaur J, Kym D, Segovia NA, et al. Innovative technique for early-onset scoliosis casting using Jackson table. Spine Deform. 2022 Nov;10(6):1461-1466.

7. Odent T, Ilharreborde B, Miladi L, Khouri N, Violas P, et al. Scoliosis Study Group (Groupe d'étude de la scoliose); French Society of Pediatric Orthopedics (SOFOP). Fusionless surgery in early-onset scoliosis. Orthop Traumatol Surg Res. 2015 Oct;101(6 Suppl):S281-8.

8. Studer D, Hasler CC. Long term outcome of vertical expandable prosthetic titanium rib treatment in children with early onset scoliosis. Ann Transl Med. 2020 Jan;8(2):25. doi: 10.21037/atm.2019.09.158.

9. Roye BD, Fano AN, Matsumoto H, Fields MW, Emans JB, et al. Pediatric Spine Study Group. The Impact of Unplanned Return to the Operating Room on Health-related Quality of Life at the End of Growth-friendly Surgical Treatment for Early-onset Scoliosis. J Pediatr Orthop. 2022 Jan 1;42(1):17-22.

10. Wijdicks SPJ, Lemans JVC, Verkerke GJ, Noordmans HJ, Castelein RM, et al. The potential of spring distraction to dynamically correct complex spinal deformities in the growing child. Eur Spine J. 2021 Mar;30(3):714-723.

11. Lemans JVC, Tabeling CS, Castelein RM, Kruyt MC. Identifying complications and failure modes of innovative growing rod configurations using the (hybrid) magnetically controlled growing rod (MCGR) and the spring distraction system (SDS). Spine Deform. 2021 Nov;9(6):1679-1689.

12. Lemans, J.V., Tabeling, C.S., Scholten, E.P. et al. Surgical treatment of neuromuscular Early Onset Scoliosis with a bilateral posterior one-way rod compared to the Spring Distraction System: study protocol for a limited-efficacy Randomized Controlled Trial (BiPOWR). BMC Musculoskelet Disord 24, 20 (2023).

13. Lebon J, Batailler C, Wargny M, Choufani E, Violas P, et al. Magnetically controlled growing rod in early onset scoliosis: a 30-case multicenter study. Eur Spine J. 2017 Jun;26(6):1567-1576.

14. Kwan KYH, Alanay A, Yazici M, Demirkiran G, Helenius I, et al. Unplanned Reoperations in Magnetically Controlled Growing Rod Surgery for Early Onset Scoliosis With a Minimum of Two-Year Follow-Up. Spine (Phila Pa 1976). 2017 Dec 15;42(24):E1410-E1414.

15. Tabeling CS, Lemans JVC, Top A, Scholten EP, Stempels HW, et al. The Spring Distraction System for Growth-Friendly Surgical Treatment of Early Onset Scoliosis: A Preliminary Report on Clinical Results and Safety after Design Iterations in a Prospective Clinical Trial. J Clin Med. 2022 Jun 28;11(13):3747.

16. Lemans JVC, Wijdicks SPJ, Koutsoliakos I, Hekman EEG, Agarwal A, et al. Distraction forces on the spine in early-onset scoliosis: A systematic review and meta-analysis of clinical and biomechanical literature. J Biomech. 2021 Jul 19;124:110571

17. Wijdicks SPJ, Lemans JVC, Verkerke GJ, Noordmans HJ, Castelein RM, et al. The potential of spring distraction to dynamically correct complex spinal deformities in the growing child. Eur Spine J. 2021 Mar;30(3):714-723.

18. de Reuver S, de Block N, Brink RC, Chu WCW, Cheng JCY, et al. Convex-concave and anterior-posterior spinal length discrepancies in adolescent idiopathic scoliosis with major right thoracic curves versus matched controls. Spine Deform. 2023 Jan;11(1):87-93.

19. Labrom FR, Izatt MT, Contractor P, Grant CA, Pivonka P, Askin GN, Labrom RD, Little JP. Sequential MRI reveals vertebral body wedging significantly contributes to coronal plane deformity progression in adolescent idiopathic scoliosis during growth. Spine Deform. 2020 Oct;8(5):901-910.

20. Brink RC, Schlösser TPC, Colo D, Vavruch L, van Stralen M, Vincken KL, Malmqvist M, Kruyt MC, Tropp H, Castelein RM. Anterior Spinal Overgrowth Is the Result of the Scoliotic Mechanism and Is Located in the Disc. Spine (Phila Pa 1976). 2017 Jun 1;42(11):818-822.

21. de Reuver S, Brink RC, Homans JF, Vavruch L, Tropp H, Kruyt MC, van Stralen M, Castelein RM. Anterior lengthening in scoliosis occurs only in the disc and is similar in different types of scoliosis. Spine J. 2020 Oct;20(10):1653-1658.

22. Aronsson DD, Stokes IA, McBride CA. Contributions of Remodeling and Asymmetrical Growth to Vertebral Wedging in a Scoliosis Model. Spine Deform. 2013 Jan;1(1):2-9.

23. Cheung WK, Cheung JPY. Contribution of coronal vertebral and IVD wedging to Cobb angle changes in adolescent idiopathic scoliosis during growth. BMC Musculoskelet Disord. 2022 Oct 10;23(1):904.

24. Newton PO, Takahashi Y, Yang Y, Yaszay B, Bartley CE, et al.. Anterior vertebral body tethering for thoracic idiopathic scoliosis leads to asymmetric growth of the periapical vertebrae. Spine Deform. 2022 May;10(3):553-561.

25. McDonald TC, Shah SA, Hargiss JB, Varghese J, Boeyer ME, et al. Harms Nonfusion Study Group. When successful, anterior vertebral body tethering (VBT) induces differential segmental growth of vertebrae: an in vivo study of 51 patients and 764 vertebrae. Spine Deform. 2022 Jul;10(4):791-797.

26. Lippross S, Grages A, Lueders KA, Braunschweig L, Austein F, Tsaknakis K, Lorenz HM, Hell AK. Vertebral body changes after continuous spinal distraction in scoliotic children. Eur Spine J. 2021 Jul;30(7):1928-1934

27. de Reuver S, Costa L, van Rheenen H, Tabeling CS, Lemans JVC, et al. Disc and Vertebral Body Morphology From Birth to Adulthood. Spine (Phila Pa 1976). 2022 Apr 1;47(7):E312-E318.

28. Stokes IA, Windisch L. Vertebral height growth predominates over intervertebral disc height growth in adolescents with scoliosis. Spine (Phila Pa 1976). 2006 Jun 15;31(14):1600-4.

29. Brink RC, Homans JF, Schlösser TPC, van Stralen M, Vincken KL, Shi L, Chu WCW, Viergever MA, Castelein RM, Cheng JCY. CT-based study of vertebral and intravertebral rotation in right thoracic adolescent idiopathic scoliosis. Eur Spine J. 2019 Dec;28(12):3044-3052.

30. Yeung KH, Man GCW, Deng M, Lam TP, Cheng JCY, et al. Morphological changes of Intervertebral Disc detectable by T2-weighted MRI and its correlation with curve severity in Adolescent Idiopathic Scoliosis. BMC Musculoskelet Disord. 2022 Jul 10;23(1):655.